Symmetry Relaxation of Three-Level Optimal Pulse Patterns for Lower Harmonic Distortion

Annika Birth[*], Tobias Geyer[†], Hendrik du Toit Mouton[*]
[*]Department of Electrical and Electronic Engineering
University of Stellenbosch
Private Bag X1, Matieland, 7602
Stellenbosch, South Africa
Email: 21519234@sun.ac.za, dtmouton@sun.ac.za

[†]ABB Corporate Research
Segelhofstrasse 1K
5405 Baden-Dättwil, Switzerland
Email: t.geyer@ieee.org

Keywords

Abstract

Pulse width modulation by optimized pulse patterns lowers the harmonic current distortions in high power converters as a result of a specifically designed optimization problem. The typically imposed quarter- and half-wave symmetry on the switching signal adds artificial restrictions to the optimization problem, which leads to suboptimal solutions. Relaxing these symmetry restrictions, a general optimization problem is formulated, which achieves up to 30 % lower harmonic distortions.

Introduction

To control the output voltage of a converter, pulse width modulation (PWM) techniques are used to translate a continuous-valued modulating signal u^* to a discrete-valued switching signal u by using a sequence of pulses of variable width. The switching nature of PWM introduces unwanted harmonic content in the converter output. Optimal PWM aims to reduce the harmonic distortions in the output by computing the pulse patterns, i.e. the switching angles, in an offline procedure. In order to simplify the harmonic representation of the pulse pattern, periodicity and quarter- and half-wave symmetry are typically imposed. This reduces the problem dimension to d switching angles in the first quarter period of the pattern.

Two distinct performance criteria are applied when calculating the switching angles of the pulse patterns. The concept of selective harmonic elimination (SHE) was first presented in 1970 [1]. The angles are determined by solving a system of d algebraic equations that eliminate $d - 1$ harmonics and set the fundamental component to the desired magnitude. In the late 1970s, a second approach was introduced that derives an optimization problem designed to minimize the entire harmonic content of the converter output, resulting in optimized pulse patterns (OPPs) [2]. This technique is sometimes also referred to as synchronous optimal PWM.

A more general approach to the SHE problem was presented in [3], which relaxes the assumption of quarter-wave symmetry for two- and three-level switching signals. Due to this relaxation, the solution space increases and multiple new solutions can be found. Research on relaxed symmetry SHE was further extended to multi-level converters [4], resulting in an infinite number of solutions.
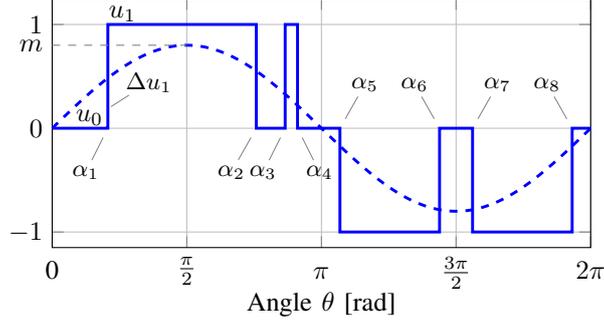
Fig. 1: Single-phase full-wave symmetric pulse pattern (solid line) with $k = 8$ switching angles α_i and switching transitions Δu_i. The fundamental component (dashed line) has the amplitude $\hat{u}_1 = m$.

For the OPP problem, the relaxation of quarter-wave symmetry was investigated only recently in [5] and [6] considering pulse numbers 5 and 7, respectively. Compared with the traditional quarter- and half-wave symmetric results, the relaxed OPPs have superior harmonic performance in certain ranges of the modulation index. In [7], OPPs with relaxed quarter-wave symmetry were computed for a two-level inverter including the different isotropy properties of the connected synchronous motor. Again, the half-wave symmetric OPPs reduce the harmonic distortions in certain intervals of the modulation range.

This paper introduces OPPs with relaxed symmetry for the three-level inverter. The general pulse pattern definitions and PWM requirements are formulated, and used to derive the optimization problems for OPPs with half-wave symmetry, and symmetry of one period, i.e. full-wave symmetry. The analysis of the relaxed OPP optimization problem reveals certain new features, such as lower harmonic distortions for specific modulation indices and OPPs with non-integer pulse numbers.

General Considerations

OPPs are the solution to a constrained optimization problem, i.e. the minimization of a cost function subject to constraints. The key characteristics of the general OPP optimization problem for a three-level neutral-point clamped (NPC) inverter are described in this section.

Switching Signal

The single-phase full-wave symmetric switching signal $u(\theta)$ is a periodic waveform defined by $k + 1$ switch positions u_i with $i \in \{0, \ldots, k\}$, and k switching angles α_i with $i \in \{1, \ldots, k\}$ over a fundamental period of 2π, see Fig. 1. For the three-level inverter, the switch positions are restricted to $u_i \in \{-1, 0, 1\}$. In fact, the switch positions in the first half-wave of the fundamental, from 0 to π, are assumed to be either 0 or 1, and accordingly either -1 or 0 in the second half-wave, from π to 2π. Due to periodicity, the initial and last switch position must be the same, which implies an even number of switching angles k.

The switching angles correspond to the *switching transitions* $\Delta u_i = u_i - u_{i-1}$ with $\Delta u_i \in \{-1, 1\}$. Owing to the distinction between the positive and negative half-wave of the pulse pattern and the restricted domain of the three-level switching signal, it follows that there is a fixed sequence of switching transitions for every k over one period.

Consider a three-level switching signal with period $T_1 = 1/f_1$ and k switching transitions. Each transition causes one of the four semiconductors in a phase-leg to turn on. This means that *on average* in one fundamental period each semiconductor has $k/4$ turn-on transitions, giving an average device switching frequency of $f_{sw} = k/(4T_1)$. The ratio of device switching frequency to fundamental frequency defines the *pulse number d*

$$d = \frac{f_{sw}}{f_1} = \frac{k}{4}. \tag{1}$$

Typically, for three-level OPPs with quarter- and half-wave symmetry, the pulse number d is an integer number. For full-wave symmetric OPPs, the number of switching angles k is restricted to even integer

numbers due to periodicity. Following the definition in (1), this gives rise to non-integer pulse numbers, e.g. $d = 1.5$ for $k = 6$.

Harmonic Analysis

A periodic signal, such as the switching signal $u(\theta)$, can be represented by the Fourier series expansion

$$u(\theta) = \frac{a_0}{2} + \sum_{n=1}^{\infty} \big(a_n \cos(n\theta) + b_n \sin(n\theta) \big). \tag{2}$$

Assuming a period of 2π, the Fourier coefficients a_n and b_n of the harmonic order n are given by

$$a_n = \frac{1}{\pi} \int_0^{2\pi} u(\theta) \cos(n\theta) \, d\theta, \quad \text{for } n \geq 0 \qquad \text{and} \qquad b_n = \frac{1}{\pi} \int_0^{2\pi} u(\theta) \sin(n\theta) \, d\theta, \quad \text{for } n \geq 1. \tag{3}$$

The amplitude $\hat{u}_n$ of the n-th switching signal harmonic is given by $\hat{u}_n = \sqrt{a_n^2 + b_n^2}$. Note that $n = 1$ denotes the fundamental component, and $n > 1$ characterizes the harmonic content of the signal.

The metric of minimal harmonic distortions in the inverter output current is adopted for the OPP computation by minimizing the total demand distortion (TDD) of the current. The TDD is the square root of the sum of the squared current harmonics $\hat{i}_n$ relative to the nominal current

$$I_{\text{TDD}} = \frac{1}{\sqrt{2} I_{\text{nom}}} \sqrt{\sum_{n \neq 1} \big(\hat{i}_n \big)^2}, \tag{4}$$

where I_{nom} is the rms value of the nominal current.

Assuming the inverter is connected to an induction machine, the current harmonics are dependent on the total stator leakage inductance L_σ, as the stator resistance can be neglected: $\hat{i}_n = \hat{v}_n / (n\omega_1 L_\sigma)$. This implies a frequency weighting of the voltage harmonics $\hat{v}_n$ with multiples of $\omega_1 = 2\pi f_1$, i.e. the fundamental angular frequency.

The harmonics of the inverter output voltage are the scaled switching signal harmonics. In case of the three-level inverter, the scaling factor is half the dc-link voltage V_{dc}: $\hat{v}_n = (V_{\text{dc}}/2)\, \hat{u}_n$. Substituting both mathematical relationships in (4) gives a closed form for the current TDD as a function of the switching signal harmonics.

$$I_{\text{TDD}} = \frac{1}{\sqrt{2} I_{\text{nom}}} \frac{V_{\text{dc}}}{\omega_1 L_\sigma} \frac{1}{2} \sqrt{\sum_{n \neq 1} \left(\frac{\hat{u}_n}{n} \right)^2} \tag{5}$$

Splitting (5) into two terms gives: $I_{\text{TDD}} = C\sqrt{J}$, where C is a constant factor depending only on the inverter and machine parameters. It is thus apparent that the term under the square root J is proportional to the current TDD. It is therefore taken as objective function for the OPP optimization problem.

$$J = \sum_{n \neq 1} \left(\frac{\hat{u}_n}{n} \right)^2 \tag{6}$$

Problem Statement

In a symmetrical three-phase system with a floating star point, voltage harmonics of triplen order, i.e. integer multiples of three, are in phase and thus have no influence on the load current. Therefore, triplen order harmonics are not considered in the objective function. Furthermore, due to symmetry between the three phases, the computation of the single-phase switching signal is sufficient.

The switching signal is defined to have zero dc-offset, a fundamental phase shift of zero and a fundamental magnitude corresponding to that of the modulating signal, i.e. the modulation index m. Furthermore,

the optimization variables, i.e. the switching angles, have to remain in ascending order and within a fundamental period.

Thus, with the only assumption of full-wave symmetry, the general OPP problem for a three-level inverter connected to an inductive load is as follows

$$
\begin{aligned}
\underset{\alpha_i}{\text{minimize}} \quad & J(\alpha_i) = \sum_{n=2,4,5,7,\dots} \frac{1}{n^2}\left(a_n^2 + b_n^2\right) \\
\text{subject to} \quad & a_0 = 0 \\
& a_1 = 0 \\
& b_1 = m \\
& 0 \le \alpha_1 \le \alpha_2 \le \dots \le \alpha_{4d} \le 2\pi.
\end{aligned}
\tag{7}
$$

The Fourier coefficients a_n and b_n are functions of the switching angles. The closed-form expressions depending on the different symmetry assumptions are derived in the following section.

Full-Wave Symmetry

In the optimization problem for OPPs with full-wave symmetry, i.e. periodicity of 2π, all $4d$ switching angles are the optimization variables. As there is no symmetry within one period, the pattern over one full period is considered to derive the Fourier coefficients. Recall that the switching signal is a piece-wise constant signal. Thus, the integrals in (3) can be split into $4d + 1$ parts with the switching angles as limits and the switch positions as constant factors

$$
a_n = \frac{1}{\pi}\left[u_0 \int_0^{\alpha_1} \cos(n\theta)d\theta + u_1 \int_{\alpha_1}^{\alpha_2} \cos(n\theta)d\theta + \dots + u_{4d} \int_{\alpha_{4d}}^{2\pi} \cos(n\theta)d\theta \right].
\tag{8}
$$

Representing the switch positions as the sum of switching transitions, $u_i = u_0 + \sum_{j=1}^{i} \Delta u_j$, allows to rearrange the integrals as follows, see in detail [8, Ch. 3 Appendix A],

$$
\begin{aligned}
a_n &= \frac{1}{\pi}\left[u_0 \int_0^{\alpha_1} \cos(n\theta)d\theta + (u_0 + \Delta u_1)\int_{\alpha_1}^{\alpha_2}\cos(n\theta)d\theta + \dots + \left(u_0 + \sum_{i=1}^{4d}\Delta u_i\right)\int_{\alpha_{4d}}^{2\pi}\cos(n\theta)d\theta \right] \\
&= \frac{1}{\pi}\left[u_0 \int_0^{2\pi}\cos(n\theta)d\theta + \Delta u_1 \int_{\alpha_1}^{2\pi}\cos(n\theta)d\theta + \dots + \Delta u_{4d}\int_{\alpha_{4d}}^{2\pi}\cos(n\theta)d\theta \right] \\
&= \frac{1}{\pi}\left[u_0 \int_0^{2\pi}\cos(n\theta)d\theta + \sum_{i=1}^{4d}\Delta u_i \int_{\alpha_i}^{2\pi}\cos(n\theta)d\theta \right].
\end{aligned}
\tag{9}
$$

Solving the integrals gives the compact form of the Fourier coefficients for full-wave symmetric pulse patterns as listed in (10) in Table I. We can see from the derived expressions that the full-wave symmetric switching signal consists of all integer order harmonics with an arbitrary phase shift and a dc-component. This requires the additional constraints in (7) on the dc-offset and the phase shift of the fundamental component.

Half-Wave Symmetry

Assuming half-wave symmetry, i.e. $u(\pi + \theta) = -u(\theta)$, restricts the switching signal optimization to one half-wave of the pattern. This means that the $2d$ switching angles are constrained to be between 0 and π and should be in ascending order. Furthermore, from half-wave symmetry follows that the signal contains only harmonics of odd order and is without dc-offset. Thus only odd, non-triplen harmonics are considered in this optimization problem, and the dc-offset constraint can be dropped, as it is satisfied for all solutions. The coefficients for the half-wave symmetry OPP problem are given in (11) in Table I.

Table I: Fourier coefficients a_n and b_n when assuming full-wave (or 2π) symmetry (FWS), half-wave symmetry (HWS), and quarter- and half-wave symmetry (QaHWS)

	a_n	b_n
FWS	$a_0 = 2u_0 - \dfrac{1}{\pi}\sum\limits_{i=1}^{4d}\Delta u_i \alpha_i$ $a_n = -\dfrac{1}{n\pi}\sum\limits_{i=1}^{4d}\Delta u_i \sin(n\alpha_i)$	$b_n = \dfrac{1}{n\pi}\sum\limits_{i=1}^{4d}\Delta u_i \cos(n\alpha_i)$ (10)
HWS	$a_n = \begin{cases} 0, & n = 0,2,4,\ldots \\ -\dfrac{2}{n\pi}\sum\limits_{i=1}^{2d}\Delta u_i \sin(n\alpha_i), & n = 1,3,5,\ldots \end{cases}$	$b_n = \begin{cases} 0, & n = 0,2,4,\ldots \\ \dfrac{2}{n\pi}\sum\limits_{i=1}^{2d}\Delta u_i \cos(n\alpha_i), & n = 1,3,5,\ldots \end{cases}$ (11)
QaHWS	$a_n = 0$	$b_n = \begin{cases} 0, & n = 0,2,4,\ldots \\ \dfrac{4}{n\pi}\sum\limits_{i=1}^{d}\Delta u_i \cos(n\alpha_i), & n = 1,3,5,\ldots \end{cases}$ (12)

Quarter- and Half-Wave Symmetry

By additionally imposing quarter-wave symmetry $u(\pi - \theta) = u(\theta)$ on the pulse pattern, the optimization problem gets further restricted to one quarter of a fundamental period with d optimization variables. The combination of quarter-wave and half-wave symmetry turns the switching signal into an odd function with only odd-order harmonics without phase shifts. As a result, the Fourier coefficients a_n and all b_n of even order are zero, see (12) in Table I. In this case, the harmonic amplitude is directly given by $\hat{u}_n = b_n$ and the optimization variables are restricted to the first quarter period $0 \leq \alpha_i \leq \frac{\pi}{2}$. This case corresponds to the traditional formulation of the OPP problem.

Results

In the following section, the effects of the symmetry relaxation on the OPP problem are shown and the resulting current TDDs are compared to the traditional OPP results. For the OPP computation, we consider a three-level NPC inverter connected to a three-phase induction machine. The system parameters are given in Table II.

The OPPs were computed for the entire modulation index range from 0 to $\frac{4}{\pi}$ with a step size of 0.01. The number of initial conditions for the optimization problem at each step was chosen as 100 to increase

Table II: System parameters

Parameter	Symbol	SI value
Rated line-to-line voltage	V_R	3.3 kV
Rated stator current	I_R	2.12 kA
Rated angular stator frequency	ω_{sR}	$2\pi 50$ rad/s
Dc-link voltage	V_{dc}	5.2 kV
Total leakage inductance	L_σ	0.73 mH
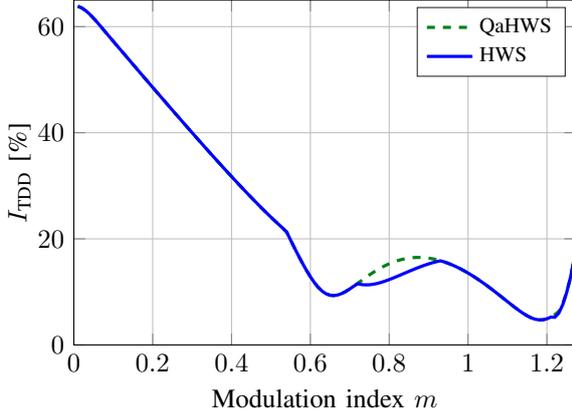
Fig. 2: Current TDDs of quarter- and half-wave symmetric (QaHWS) OPPs and half-wave symmetric (HWS) OPPs with $d = 2$
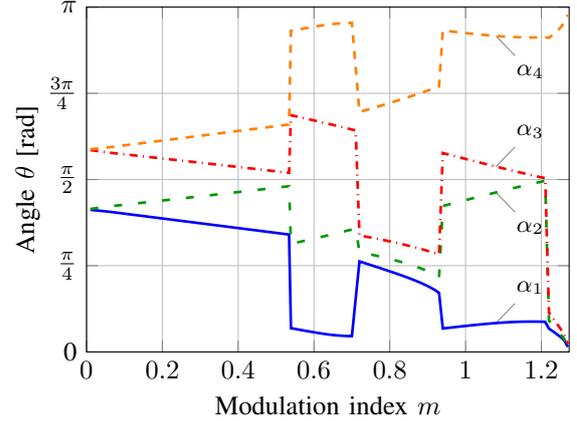
Fig. 3: Switching angles in the first half-wave of the half-wave symmetric OPPs with $d = 2$

the probability of finding the global minimum. The infinite sum of harmonics in the objective function is approximated by considering the first 100 harmonics. This is justified by the fact that the harmonic magnitudes at high frequencies are very small. The computation was done for pulse numbers 2 and 3. In the case of full-wave symmetry, the pulse numbers 1.5 and 2.5 were also considered. The computation of the OPPs was done with the `fmincon` solver of the MATLAB Optimization Toolbox™.

For pulse number 2, the current TDDs of OPPs with quarter- and half-wave symmetry and only half-wave symmetry imposed are compared in Fig. 2. The figure shows that, in certain intervals of the modulation index, the current TDD is reduced by the half-wave symmetric OPPs. In the remaining modulation index ranges, the half-wave symmetric problem yields the same results as the traditional quarter- and half-wave symmetric problem. The limits of the improvement intervals and the maximum improvement in absolute value and percentage of the original current TDD are listed in Table III.

The change from quarter- and half-wave symmetry to only half-wave symmetry in the improvement intervals is also apparent from Fig. 3. The figure shows the solutions to the half-wave symmetry optimization problem, which is the set of switching angles in the first half-wave. We can see from the figure that for all modulation indices except within the improvement intervals, the four switching angles are symmetric to each other with respect to $\frac{\pi}{2}$. For modulation indices within the improvement intervals, the third switching angle is shifted below $\frac{\pi}{2}$, which eliminates the quarter-wave symmetry.

From Fig. 2 and Table III, we can see that the current TDD can be reduced by up to 20 % with half-wave symmetric OPPs. This highlights the fact that the commonly imposed quarter-wave symmetry assumption is in fact a restriction on the OPP optimization problem, which has an impact on the optimality of the solutions.

This effect of the restrictions on the optimization problem, in particular on the cost function, is visualized in Fig. 4. The figure shows the cost function of the half-wave symmetric OPP problem with pulse number 2 at the modulation index $m = 0.92$ over the entire feasible area as a function of the first α_1 and last optimization variable α_4. The remaining two optimization variables are then determined by the two constraints on the fundamental amplitude $b_1 = m$, and phase shift $a_1 = 0$. The optimal solution to the

Table III: Intervals of current TDD improvement when relaxing symmetry for $d = 2$

Interval	Modulation index interval	Maximum absolute reduction of current TDD	Maximum relative reduction of current TDD
1.	$0.72 < m < 0.93$	2.34 %	19.52 %
2.	$1.22 < m < 1.26$	0.58 %	8.60 %
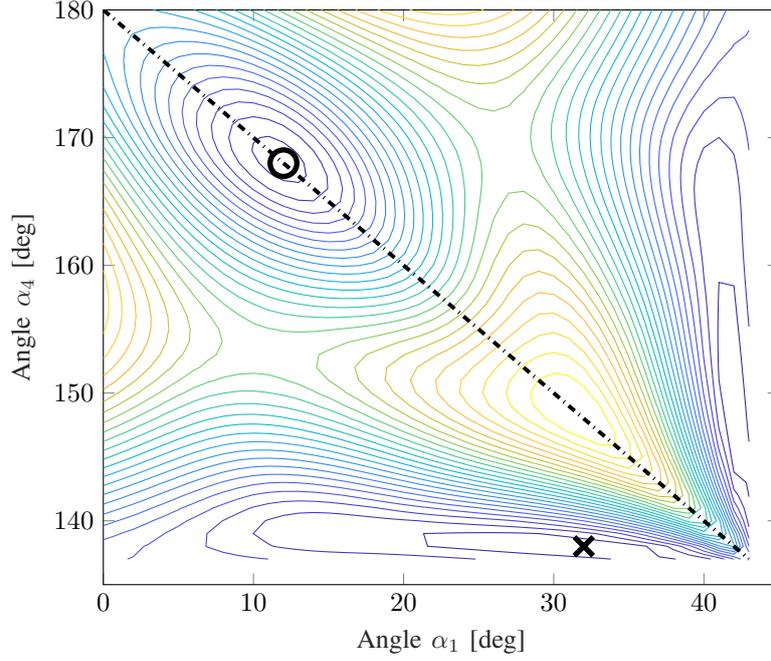
Fig. 4: Cost function in α_1 and α_4 of the half-wave symmetric OPP problem with $d = 2$, $m = 0.92$. The cross indicates the half-wave symmetry optimal solution; the circle marks the traditional optimal solution. The dashed line corresponds to the restricted solution space of the traditional problem.
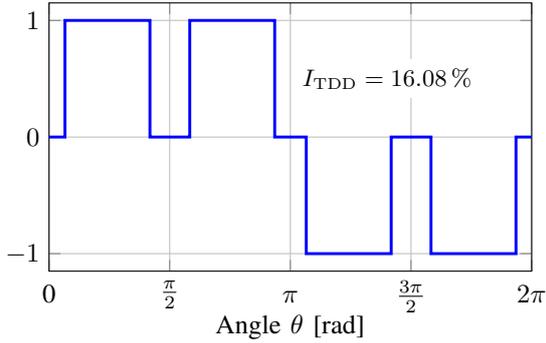
Fig. 5: Quarter- and half-wave symmetric OPP with $d = 2$, $m = 0.92$ (corresponding to the circle).
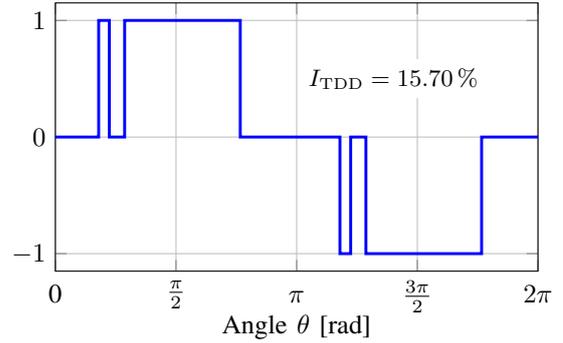
Fig. 6: Half-wave symmetric OPP with $d = 2$, $m = 0.92$ (corresponding to the cross).

problem, i.e. the global minimum, thus lies within the shown solution space. The dashed line in the figure represents the restriction due to quarter-wave symmetry, i.e. $\alpha_4 = \pi - \alpha_1$. Note that we chose the domain of the switching angles here in degree instead of radians for better readability.

For the example pulse number $d = 2$, we can see from the figure that the solution space becomes one-dimensional when imposing quarter-wave symmetry. Thus, the local minima indicated by the circle defines the optimal solution to the quarter- and half-wave symmetric OPP problem. When removing the quarter-wave symmetry restriction, the solutions space increases to the entire two-dimensional area shown in the figure. We can see that two new local minima emerge: one at the bottom and another one at the right side of the solution space. At this particular modulation index, the local minima on the bottom indicated with the cross is identified as the global minimum and thus as the optimal solution to the half-wave symmetric OPP problem.

As the modulation index is increased, the different local minima vary in magnitude. Thus, the global minimum changes along the modulation range. Each change of the global minimum corresponds to additional discontinuities of the switching angles in Fig. 3.
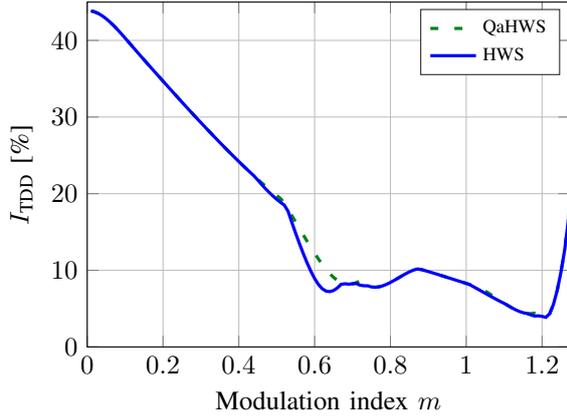
Fig. 7: Current TDDs of quarter- and half-wave (QaHWS) and half-wave symmetric (HWS) OPPs with $d = 3$.
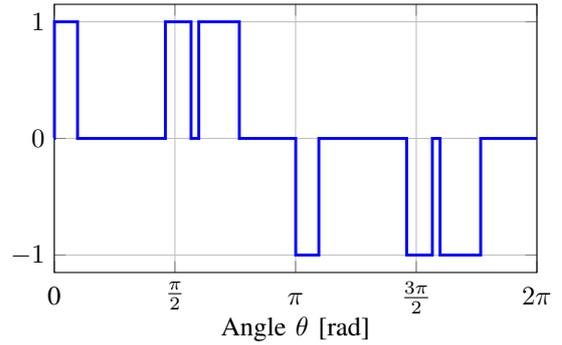
Fig. 8: Half-wave symmetric OPP with $d = 3$ and $m = 0.52$.

The resulting OPPs of the two symmetry cases for the example of $m = 0.92$ and pulse number 2 are shown in Fig. 5 and Fig. 6. We can see from the figures that the half-wave symmetric OPP achieves the lower current TDD by bringing more than half of the switching angles of one half-wave together in one quarter. This is in line with the previous observation from Fig. 3 that the third switching angle is shifted below $\frac{\pi}{2}$.

For pulse number 3, the current TDDs of the OPPs with quarter- and half-wave symmetry and only half-wave symmetry imposed are shown in Fig. 7. The symmetry relaxation again leads to improvements of the current TDD in certain intervals of the modulation index. In Table IV, the exact percentages of the current TDD reductions are listed for each interval. By relaxing quarter-wave symmetry, a relative improvement of up to 30 % of the current TDD is achieved. In the third and fourth interval, the current TDD reduction is achieved, similar as for pulse number 2, by bringing more than half of the switching angles in one half-wave together in one quarter. In the first two intervals, entirely new OPPs are the result. An example of such an OPP is shown in Fig. 8 for $m = 0.52$.

Lastly, both quarter- and half-wave symmetry are relaxed. This leads to no further reduction of the current TDD, at least for the investigated pulse numbers 2 and 3. The solutions of these full-wave symmetric optimization problems correspond for the entire modulation range to the half-wave symmetric OPPs. However, full-wave symmetry offers the feature of non-integer pulse numbers. The current TDDs of OPPs with pulse numbers 1.5 and 2.5 are shown in Fig. 9 together with the ones of the half-wave symmetric OPPs with the integer pulse numbers 1, 2 and 3. We can see from the figure that the non-integer optimization problems are feasible over the entire modulation range. Moreover, for every modulation index, there exists a full-wave symmetric OPP with a non-integer pulse number d that yields a current TDD bounded by the ones of the integer pulse numbers $\underline{d}$ and $\overline{d}$. Note that $\underline{d}$ is the next lower integer of d, while $\overline{d}$ corresponds to the next higher integer number.

In Fig. 10, an example of a full-wave symmetric OPP with pulse number $d = 2.5$ for $m = 0.9$ is shown. We can see that both half-waves are no longer symmetrical to each other, which results in an entirely new

Table IV: Intervals of current TDD improvement when relaxing symmetry for $d = 3$

Interval	Modulation index interval	Maximum absolute reduction of current TDD	Maximum relative reduction of current TDD
1.	$0.45 \le m \le 0.67$	1.96 %	29.46 %
2.	$0.71 \le m \le 0.73$	0.40 %	6.67 %
3.	$1.01 \le m \le 1.10$	0.33 %	4.35 %
4.	$1.17 \le m \le 1.19$	0.44 %	8.67 %
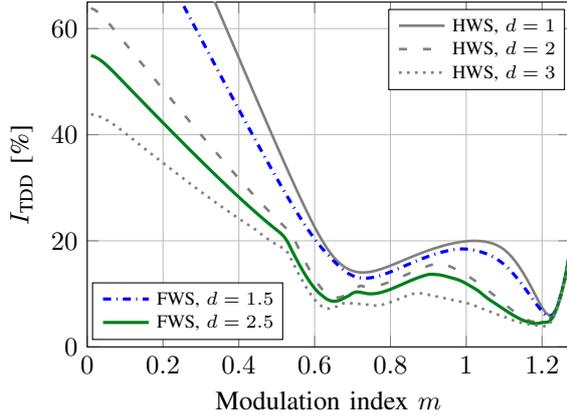
Fig. 9: Current TDDs of integer and non-integer pulse numbers.
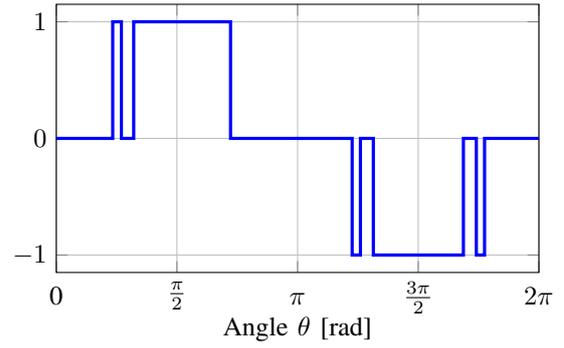
Fig. 10: Full-wave symmetric OPP with $d = 2.5$ and $m = 0.9$.

OPP. However, comparison to the OPP in Fig. 6 reveals that the first half-wave of the full-wave symmetric OPP, which comprises two pulses, closely corresponds to one half-wave of the half-wave symmetric OPP with pulse number 2. Similarly, the second half-wave of the full-wave symmetric OPP matches the half-wave of the half-wave symmetric OPP with pulse number 3. Thus, the full-wave symmetric OPP with the non-integer pulse number d is a combination of the half-wave symmetric OPPs with pulse numbers $\underline{d}$ and $\overline{d}$.

Conclusion

Relaxing quarter- and half-wave symmetry for the three-level OPP problem reveals the highly restrictive nature of these symmetry assumptions. Multiple new solutions are found for the newly derived problems with relaxed symmetry. In certain intervals of the modulation range, these new OPPs reduce the current TDD and therefore outperform the traditional suboptimal quarter- and half-wave symmetric OPPs.

In particular, relaxation of quarter-wave symmetry reduces the harmonic distortions by up to 20 % for pulse number 2 and by up to 30 % for pulse number 3. Relaxing additionally half-wave symmetry removes the restriction of integer pulse numbers. The resulting OPPs achieve current TDDs between the current TDDs of the traditional integer OPPs.

References

[1] H. S. Patel and R. G. Hoft, "Generalized techniques of harmonic elimination and voltage control in thyristor inverters: Part I–Harmonic Elimination," *IEEE Transactions on Industry Applications*, vol. IA-9, pp. 310–317, May 1973.

[2] G. S. Buja and G. B. Indri, "Optimal pulsewidth modulation for feeding AC motors," *IEEE Transactions on Industry Applications*, vol. IA-13, pp. 38–44, Jan. 1977.

[3] J. R. Wells, B. M. Nee, P. L. Chapman, and P. T. Krein, "Selective harmonic control: A general problem formulation and selected solutions," *IEEE Transactions on Power Electronics*, vol. 20, pp. 1337–1345, Nov. 2005.

[4] W. Fei, X. Du, and B. Wu, "A generalized half-wave symmetry SHE-PWM formulation for multi-level voltage inverters," *IEEE Transactions on Industrial Electronics*, vol. 57, pp. 3030–3038, Sep. 2010.

[5] A. Tripathi and G. Narayanan, "Optimal pulse width modulation of voltage-source inverter fed motor drives with relaxation of quarter wave symmetry condition," in *IEEE International Conference on Electronics, Computing and Communication Technologies (CONECCT)*, Jan. 2014.

[6] A. Tripathi and G. Narayanan, "High-performance off-line pulse width modulation without quarter wave symmetry for voltage-source inverter," in *International Conference on Advances in Electronics Computers and Communications*, Oct. 2014.

[7] A. D. Birda, J. Reuss, and C. Hackl, "Synchronous optimal pulse-width modulation with differently modulated waveform symmetry properties for feeding synchronous motor with high magnetic anisotropy," in *European Conference on Power Electronics and Applications (EPE'17 ECCE Europe)*, Sept. 2017.

[8] T. Geyer, *Model Predictive Control of High Power Converters and Industrial Drives*. Wiley, 2016.